# Proton transport in biological systems can be probed by two-dimensional infrared spectroscopy

Chungwen Liang, Thomas L. C. Jansen, and Jasper Knoester
*Center for Theoretical Physics and Zernike Institute for Advanced Materials, University of Groningen, Nijenborgh 4, 9747 AG Groningen, The Netherlands*

(Received 30 August 2010; accepted 9 November 2010; published online 24 January 2011)

We propose a new method to determine the proton transfer (PT) rate in channel proteins by two-dimensional infrared (2DIR) spectroscopy. Proton transport processes in biological systems, such as proton channels, trigger numerous fundamental biochemical reactions. Due to the limitation in both spatial and time resolution of the traditional experimental approaches, describing the whole proton transport process and identifying the rate limiting steps at the molecular level is challenging. In the present paper, we focus on proton transport through the Gramicidin A channel. Using a kinetic PT model derived from all-atom molecular dynamics simulations, we model the amide I region of the 2DIR spectrum of the channel protein to examine its sensitivity to the proton transport process. We demonstrate that the 2DIR spectrum of the isotope-labeled channel contain information on the PT rate, which may be extracted by analyzing the antidiagonal linewidth of the spectral feature related to the labeled site. Such experiments in combination with detailed numerical simulations should allow the extraction of site dependent PT rates, providing a method for identifying possible rate limiting steps for proton channel transfer. © *2011 American Institute of Physics*. [doi:10.1063/1.3522770]

## I. INTRODUCTION

Proton transport is a chemical process that is essential for maintaining cellular life. It plays an important role in photosynthesis, enzyme catalysis, acid-base neutralization, etc. The proton transport process in water differs from the typical mass diffusion of ion transport in solutions. The former takes place via the Grotthuss mechanism,[1,2] which makes the proton conductivity significantly larger than the ion conductivity.[3] This mechanism involves that a proton hops from the hydronium ion to an adjacent water molecule by interconversion of a hydrogen bond and a covalent bond. Thus, the charge of the proton is transferred. In bulk water the extended hydrogen bonding network is important for the efficiency of the proton transfer (PT) process.[4] When PT takes place in a system in which the number of surrounding water molecules is limited, for instance, for protons confined inside micelles or transmembrane protein channels, it is different from the PT process in bulk water and other factors than the local hydrogen bond network will play an essential role in determining the PT process. A schematic picture of PT in bulk water and in channel water is shown in Figs. 1(a) and 1(b), respectively.

The peptide gramicidin A (gA) is one of the best-characterized prototypic transmembrane protein channels, and has been the subject of a large amount of experimental[5–8] and theoretical[9–13] studies. It plays an important role in proton/ion transport through the cell membrane. The antibiotic activity of the gA channel is a result of increasing the permeability of inorganic monovalent cations through the bacterial cell membrane, thereby destroying the ion gradient between the cytoplasm and the extracellular environment.[14] The primary structure consists of 15 alternating D- and L-amino acids. The active peptide forms a $\beta$-helical dimer with a hydrophilic narrow pore (diameter ~0.4 nm) in the center, allowing a single-file water chain to penetrate. Therefore, under this condition, the water diffusion and rotation mechanisms must play crucial roles in ion and proton transport.[10,15–17] It has been suggested that the PT process in the channel relates to two mechanisms: proton hopping and water reorientation.[11,17–19] After a proton translocates from one side of the channel to the other through the single-file water chain via the Grotthuss mechanism, all the water molecules will have changed their orientations [Fig. 1(c)]. If a proton should transport along the same direction again, all the water molecules must first flip back to accommodate this proton. The proton entering or leaving the channel[11,20,21] are also possible rate limiting steps. Which factor determines the overall PT rate is still debated.[15–17,19,22] To summarize, the possible bottlenecks for the proton transport through protein channels are proton hopping between water molecules, water reorientation, water diffusion, and the proton entering and leaving the channel.

The proton transport process in channels has been investigated both experimentally[8,23] and theoretically[10,12,15,16,19,24–26] to get a better understanding of the overall process. The theoretical studies have focused on water diffusion in nano-pores with classical molecular dynamics (MD) simulations[12,24,25] and proton hopping processes with *ab initio* MD,[10,15,16] multi-state empirical valence bond (MS-EVB) methods[19,26] and Monte Carlo simulations.[19] However, there is still a gap between theoretical calculations and experiments. The complete proton transport process is still not well-characterized,[27] because the available experimental tool, single channel current measurement,[8,23] only allows the extraction of the overall PT rate. Presently it is therefore not possible to distinguish between the different bottlenecks for proton transport through channel proteins.

 

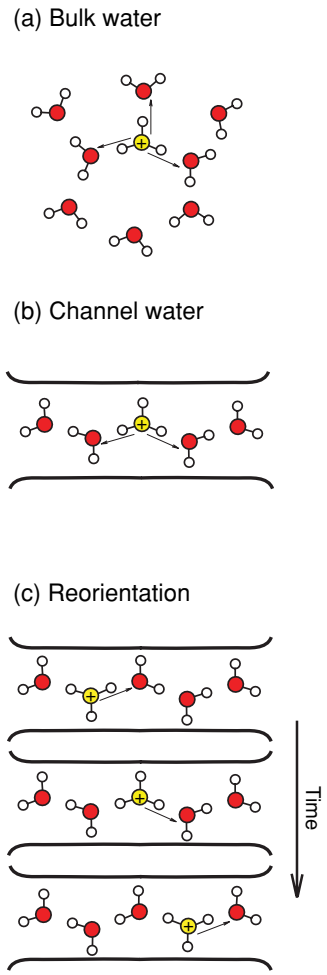


FIG. 1. Schematic figure of (a) the PT in bulk water, (b) the PT in channel water, and (c) the channel water reorientation after PT.

This paper aims at illuminating this problem. In particular, we investigate to what extent two-dimensional infrared spectroscopy (2DIR) may be used to obtain information on the intermolecular PT rate inside the gA channel. Recent studies[28–34] have demonstrated the potential of 2DIR to probe molecular scale processes, such as structural dynamics and energy transfer, in a complex molecular environment at time scales down to pico- and femtoseconds. The optically strongly active C=O stretch vibration (the amide I mode), which occurs in many organic molecules, is the most popular excitation used in 2DIR. The 2DIR experiment can probe accurately how the fluctuating environment, in particular its charge distribution, affects the vibrational frequency through the Stark effect. For the problem at hand, the surmise is that the charge of the moving proton (along with other dynamics in the channel) is reflected in fluctuations of the C=O vibrational frequency in the carbonyl groups of the gA peptide forming the channel. By isotope labeling specific C=O groups, this information may be made site specific, because it allows for spectral separation of this particular site from contributions caused by the other amide I vibrations in the channel.[35–39]

The analysis of 2DIR experiments currently relies on molecular dynamics (MD) simulations to obtain structural information, and *ab initio* maps to translate this information into a time-dependent vibrational model Hamiltonian.[40] Solving the time-dependent Schrödinger equation for this Hamiltonian then yields the linear infrared absorption and 2DIR spectra.[41] For the problem of proton transport through the gA channel, following the above modeling strategy is computationally too expensive. The reason is that the presence of the proton requires high-level proton simulation methods, such as Car–Parrinello molecular dynamics (CPMD), which is too time-consuming to sample enough configurations for simulating the 2DIR spectrum. To circumvent this poblem, we devise a kinetic model for the proton transport that takes into account the moving proton as well as the dynamics of all molecules in the system (the water molecules, the gA protein, and the molecules that make up the membrane). We derive and parametrize the effects of the latter three contributions in the kinetic model by fitting results obtained from all-atom MD simulations and *ab initio* mapping on the channel without proton. We then add the proton, describing its hopping through a stochastic process characterized by an intermolecular transfer rate. The 2DIR spectra calculated using this approach shows that this rate is reflected in the waiting time ($t_2$) dependence of these spectra. While the proposed coarse grained model of course does not account for every possible aspect of the proton transport process, it does account for the most important parts and it gives a strong indication that extraction of the PT rate from 2DIR spectra is possible.

The remainder of this paper is organized as follows. In the Theory section we will briefly describe the all-atom MD simulations that will later be used to parameterize the kinetic PT model developed to describe the proton transport process. Next, the method for simulating the 2DIR spectra is outlined and the kinetic PT model is described. In Sec. III we first describe the results of the all-atom MD simulations and then those of the PT model, where we will focus on the possibility of extracting the proton hopping rate from 2DIR spectra of isotope labeled gA. In the end it will be discussed, how our results can be used in the study of the overall proton transport mechanism and finally conclusions will be drawn.

## II. METHODS

### A. All-atom molecular dynamics simulations

All-atom MD simulations are performed using the GROMACS 3.3.3 package[42] with the OPLS-AA force field[43] for the protein, the modified Berger's force field[44] for the lipids, and the TIP4P model[45] for the water molecules. The gA helical-dimer structure is taken from the NMR structure provided in the PDB file 1JNO.[46] The gA channel is embedded inside a bilayer of 64 DMPC lipid molecules by using Kandt's method[47] and solvated with ~2300 water ($H_2O$) molecules (as shown in supplementary Fig. 1).[48] All further details on the MD simulations are described in the supplementary information.[48]

### B. 2DIR spectrum modeling without proton

The time-dependent Hamiltonian of one isotope labeled C=O oscillator in a peptide chain reads:

$$H(t) = \omega(t)B^{\dagger}B - \frac{\Delta}{2}B^{\dagger}B^{\dagger}BB + \vec{\mu}(t)\cdot\vec{E}(t)[B^{\dagger} + B] \quad (1)$$

where $B^{\dagger}$ and $B$ are Bosonic creation and annihilation operators, respectively, of the isotope labeled oscillator. Furthermore, $\omega(t)$ is its vibrational frequency, $\vec{\mu}(t)$ is the transition dipole responsible for the coupling to the applied laser field $\vec{E}(t)$, and $\Delta = 16\ \mathrm{cm}^{-1}$ is the anharmonicity. The latter accounts for the fact that the energy gap between the single and double excited vibrational states is smaller than that between the ground state and the single excited state. The vibrational frequency is affected by the fluctuating local environment. The effect of the neighboring amide units in the peptide chain is accounted for with a dihedral map obtained from *ab initio* calculations on glycinedipeptide.[49] The frequency changes induced by the remaining environment is determined with an electrostatic map, which considers the effect of a local electric field and the electric field gradient.[40] We thus have:

$$\omega_i = \omega_{\mathrm{gas}} + \Delta\omega_N(\varphi_{i,i-1}, \psi_{i,i-1}) + \Delta\omega_C(\varphi_{i,i+1}, \psi_{i,i+1}) + \Delta\omega_{\mathrm{map}}(E(r), \nabla E(r)), \quad (2)$$

where $\omega_{\mathrm{gas}}$ is the gas phase frequency ($1717\ \mathrm{cm}^{-1}$), $\Delta\omega_N$ is the frequency shift originating from the previous site $i$-1 toward the N terminus, while $\Delta\omega_C$ is the frequency shift originating from the next site $i+1$ toward the C terminus. $\Delta\omega_{\mathrm{map}}$ is the frequency shift due to the electric field generated by surrounding protein, lipid, and water molecules.[40] The transition dipole $\vec{\mu}(t)$ fluctuates with the orientation of the isotope labeled C=O group, as well as with the local electric field and electric field gradient.[40]

Using all-atom MD simulations, the local structure of the peptide chain, lipids, and the surrounding solvent is known, and by using the above mapping, this information suffices to construct the time-dependent Hamiltonian for an oscillator in a fluctuating environment. From this Hamiltonian, linear absorption and 2DIR spectra are calculated by using the numerical integration of the Schrödinger equation (NISE) method.[41] The latter is based on numerically solving the time-dependent Schrödinger equation for the vibrational Hamiltonian $H(t)$ and using the solution to calculate optical response functions. The Schrödinger equation for the time-dependent Hamiltonian is solved numerically by successive propagation during time intervals that are short enough for the Hamiltonian to be considered constant, i.e., shorter than the time scale of the frequency fluctuations. In practice, it turns out that time intervals of 20 fs are short enough for this purpose.[30,41] The time domain response functions governing the 2DIR signal are then calculated by averaging over multiple starting configurations. The frequency domain spectra are calculated as a double Fourier transform of the time domain response functions.

### C. Kinetic PT model

We construct a PT model for a one-dimensional file of water in a gA channel, which accounts for water molecule rotation, water molecule diffusion, and the proton hopping process. We suppose that there are nine water molecules inside the gA channel according to the number (7–9) suggested by

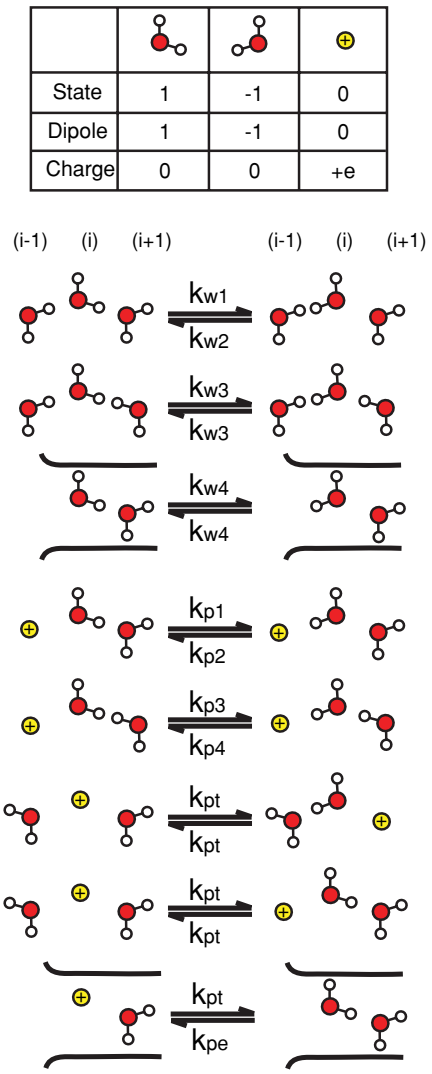


FIG. 2. Schematic figure of the states of the water molecules in the PT model (top) and list of all rate constants that describe the different processes accounted for in our kinetic model. ⊕ represents the hydronium ion, $k_{\mathrm{w4}}$ relates to water rotation in the channel entrance, and $k_{\mathrm{pe}}$ relates to the proton entering the channel.

the present all-atom simulation and previous simulations,[12] and each water molecule has three possible states: S = 1 represents a water molecule that has a positive dipole moment component along the Z direction (along the channel axis); S = −1 refers to a water molecule with a negative dipole moment component along the Z direction; S = 0 represents the protonated state, i.e., the hydronium ion with charge +e, but without a dipole component along the channel axis. These states are illustrated in Fig. 2. The justification for defining these three states for each water molecule is discussed in Sec. III.

First, we assume that the dynamics of the state of each water molecule $i$ only depends on its neighbors $i-1$ and $i+1$, and that the evolution of the states can be described by a kinetic model. In the schematic diagram shown in Fig. 2, all rotation and proton hopping processes involved are illustrated. The PT rate $k_{\mathrm{pt}}$ for proton hopping between two neighboring water molecules, will be used as an adjustable parameter in the simulations. The possibility to probe $k_{\mathrm{pt}}$ by using 2DIR is the main issue addressed in this paper, which we do

by calculating 2DIR spectra for various values of $k_{pt}$. When there is no proton inside the channel, one can enter from either side of the channel, determined by the proton entry rate $k_{pe}$, which depends on the $p$H value of the surrounding bulk water. The details related to water diffusion are described in the supplementary material.[48]

Second, the vibrational frequency of the isotope labeled C=O oscillator is modeled as:

$$\omega_{c=o} = \omega_{gas} + \Delta\omega_{protein} + \Delta\omega_{proton} + \Delta\omega_{water} + \Delta\omega_{lipid}, \quad (3)$$

where $\omega_{gas}$ is the gas-phase frequency (1717 $cm^{-1}$) of a carbonyl group and $\Delta\omega_{protein}$, $\Delta\omega_{proton}$, $\Delta\omega_{water}$, and $\Delta\omega_{lipid}$ are frequency shifts that originate from protein, proton, water, and lipid contributions, respectively. The origin of this equation is the same as Eq. (2): $\Delta\omega_{protein}$ describes the effect of the neighboring protein units, while $\Delta\omega_{proton}$, $\Delta\omega_{water}$, and $\Delta\omega_{lipid}$ are the frequency shifts induced by the electric fields caused by the proton, the water molecules, and the lipid molecules, respectively. The important difference is that Eq. (2) relies on atomic information obtained from the all-atom MD simulations, while in the kinetic model Eq. (3) all shifts are represented by stochastic coarse grained models, where the statistical properties of $\Delta\omega_{protein}$, $\Delta\omega_{water}$, and $\Delta\omega_{lipid}$ are determined by fitting to the results of the all-atom simulation for the channel in the absence of a proton (see supplementary material).[48] We choose the C=O group on the fourth residue alanine (near channel center) in the all-atom simulation for the PT model parameterization. The position of the proton is determined by allowing it to move between the various water molecules governed by a kinetic model characterized by the fixed transfer rate $k_{pt}$. The transition dipole of the isotope labeled site $\vec{\mu}$ is treated as a fixed vector along the channel axis. This approximation is justified by the observation made in the all-atom simulations that it always aligns with the Z direction and does not fluctuate much. The details of the parametrization of the kinetic model are presented in the supplementary material.[48]

Third, having obtained all details of the kinetic coarse grained model, we then generate several 1 $\mu$s trajectories with different $k_{pt}$ values for analysis and spectral simulation. The quality of the kinetic model is illustrated by comparing these spectra to those obtained from the all-atom simulations (supplementary material).[48] It should be noted that this amount of data needed for the spectral simulations could never be obtained with high-level simulation methods for the proton motion, such as CPMD.[15,50] While a single transfer event takes about 1 ps, the simulation of numerous occurrences of such an event is needed to obtain a proper ensemble average. After calculating the C=O vibrational frequency as a function of time, both linear absorption and 2DIR spectra are calculated with the NISE method.[41]

## III. RESULTS

### A. All-atom molecular dynamics simulations

The simulated system contains three different components: protein, water, and lipid. In general, the electric field

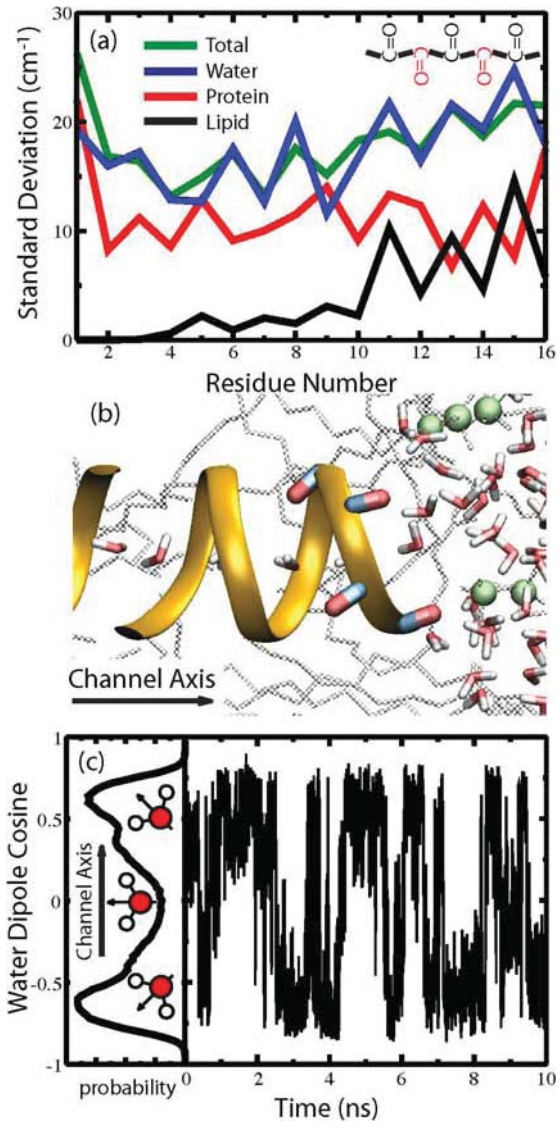


FIG. 3. The results of all-atom MD simulations of a channel without proton: (a) The standard deviation of the frequency fluctuation due to various contributions as a function of residue number. The insert shows the alternating arrangement of the C=O groups along the peptide backbone. (b) Illustration of the C=O groups close to the channel entrance (carbon: thick blue stick, oxygen: thick red stick) that are affected by lipid head groups (green spheres) and water molecules (oxygen: thin red stick, hydrogen: thin white stick). (c) The average projection of the water dipole along the channel axis as a function of time. The probability distribution of the projection is shown in the left part of the figure.

generated by each component surrounding a C=O group makes a contribution to the vibrational frequency. In order to understand the influence of the individual components, we calculate the standard deviation of the frequency shift generated by each of them and their total as a function of residue number along the channel axis. The residue number is counted from the peptide N-terminus near the channel center to the C-terminus close to channel entrance. The results are shown in Fig. 3(a). This shows that the lipid molecules make a negligible contribution in the middle of the channel (residues 1 to 10), because of the non-polar properties of the lipid tail. However, due to the polar head groups, the lipid molecules produce a large contribution for the residues close to the

channel entrance. They generate a "zigzag" contour from residue 11 to 16, because of the alternating arrangement of the C=O groups along the protein backbone [Fig. 3(b)]. The standard deviation of the frequency shift increases with the decrease of the distance between the C=O group and the lipid head groups.

The standard deviations of the protein contributions are around 10 $cm^{-1}$ on average, and have a zigzag contour close to the channel entrance in the inverse way of the lipid contribution. The C=O groups pointing into the membrane have a higher frequency spread than those pointing outward, due to the hydrogen bonding within the protein backbone. The water contribution, in general, has the same propensity as the lipid contribution near the channel entrance, but it is still significant in the middle of the channel, which can be attributed to the single file water chain inside the pore. From the results discussed above, we see that for the C=O groups located near the center of the channel (which will be our main interest), we can neglect the lipid contribution and only need to take into account the protein and water dynamics.

To understand the water behavior inside the channel, we calculate the orientation of the water molecules as a function of simulation time, as shown in Fig. 3(c). We define $\theta$ as the angle between the water dipole and the channel axis, and calculate the average of cos $\theta$ of all the water molecules inside the channel. It is easy to define two dominant orientational states of the water wire: either with positive or negative dipole components along the channel axis. The transition state (cos $\theta \sim 0$) has a relatively low probability. The reorientation time (duration of the persistence in one state) is ~500 ps, and the transition time (duration of the change from one state to the other) is ~40 ps as calculated from the simulation trajectories (total 100 ns). Here we use the definition that a reorientation event happens, when the average cos $\theta$ changes from a value larger than 0.7 to a value smaller than −0.7, or the other way round. In a previous study, it was observed that a single transition event in which all the water dipoles flipped from one orientation to the other lasted 80 ps during a 1.4 ns trajectory.[20] This shows that the motion is collective and that under confined conditions water molecules prefer to keep the same orientation. The duration of the change between orientations is considerably faster than the lifetime of the orientational states.

To sum up, the above statistical information gives insight into the dynamics of water inside the protein channel and defines the requirements that a PT model must fulfill to give a realistic description. In particular, it justifies our model with two possible orientations ($S = \pm 1$) of a neutral water molecule.

### B. Kinetic PT model

We now introduce a proton in the PT model (98% snapshots with a proton inside the channel). We examine the effect of the PT rate on the frequency fluctuations and the 2DIR spectra by using four different values: $k_{pt} = 0.1$, 0.2, 1.0, and 2.0 $ps^{-1}$. The various frequency fluctuation auto-correlation functions, $C(t)$, are plotted in Fig. 4. Comparing the correlation functions obtained accounting for the three different contributions separately (proton, water, and protein), we observe that the proton dominates the frequency memory; the lower the PT rate, the slower the frequency correlation decays. The fast protein dynamics is seen in the fast initial decay of the correlation function shownin Fig. 4(c) and is independent of the PT rate. The water and proton frequency shifts are anticorrelated with a correlation coefficient of −0.48, showing that the water molecules are screening the proton.

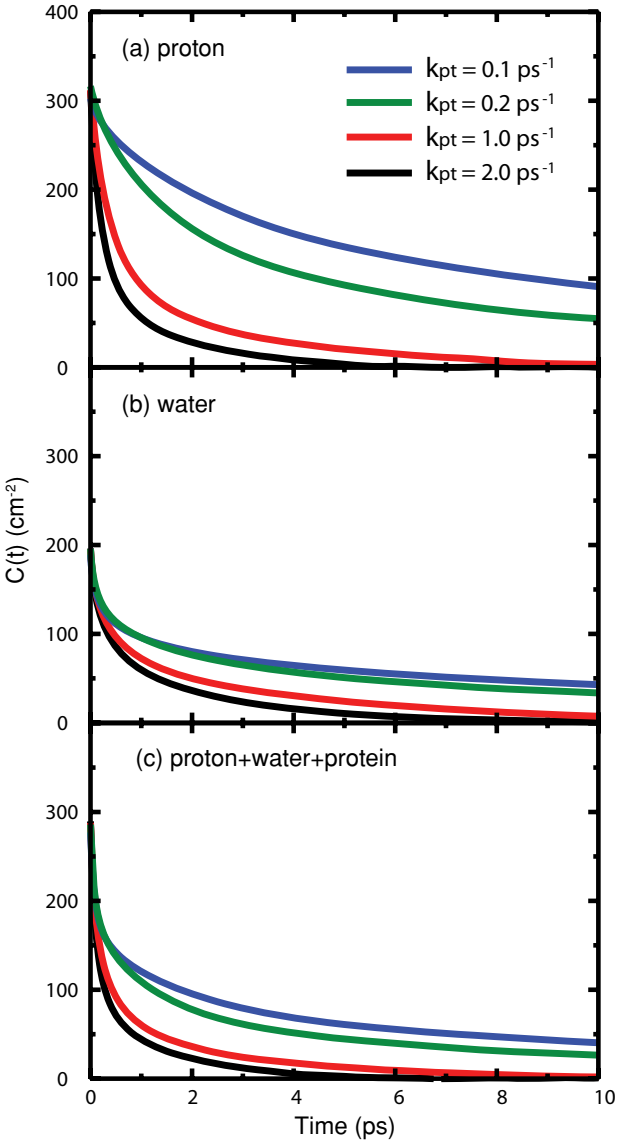


FIG. 4. The auto-correlation function of the frequency fluctuation for different $k_{pt}$ values: (a) proton contribution, (b) water contribution, and (c) including all the contributions (proton+water+protein).

2DIR experiments can be used to extract information about the frequency fluctuation auto-correlation functions. The 2DIR spectrum of the isolated isotope label contains two peaks. The diagonal peak consists of ground state bleach and stimulate emission contributions, while the peak below the diagonal arises from the excited state absorption,[38] which occurs at lower frequencies due to the anharmonicity. In general, the shape of the peaks in a 2DIR spectrum is determined by the magnitude and time scale of the frequency fluctuations.[31,51–53] If the vibrational frequencies do not have

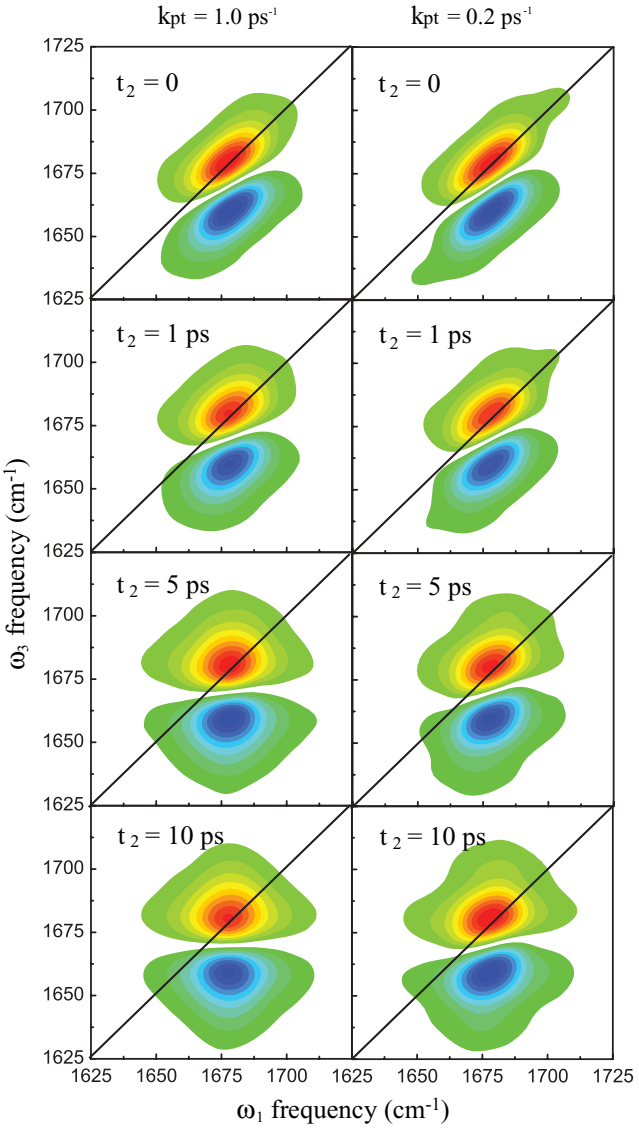


FIG. 5. The 2DIR spectra for the isotope labeled site within the PT model with $k_{pt} = 1$ ps$^{-1}$ (left column) and with $k_{pt} = 0.2$ ps$^{-1}$ (right column) at different waiting times. Each color contour represents 5% of the maximal amplitude.

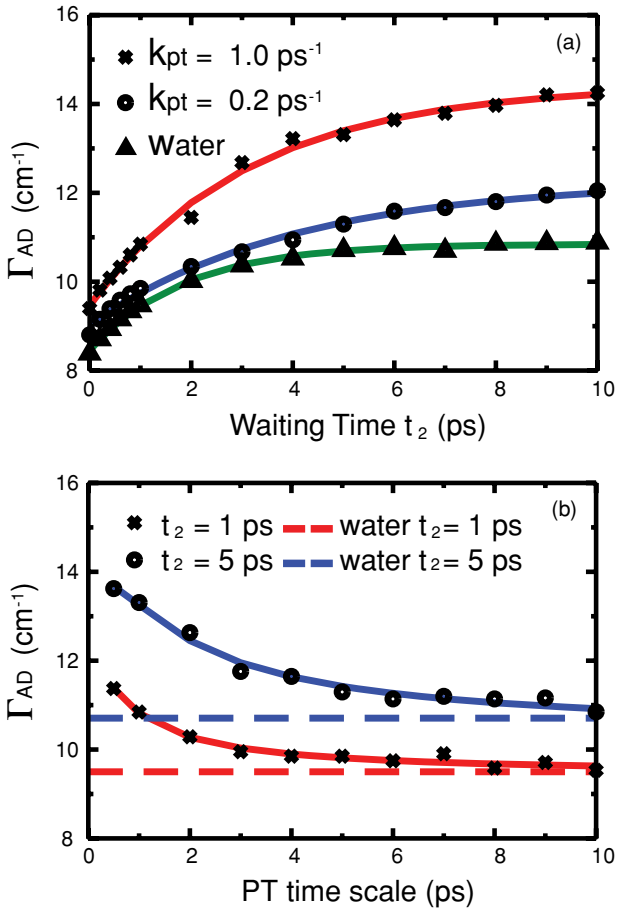


FIG. 6. Antidiagonal linewidths $\Gamma_{AD}$ of the isotope label 2DIR spectra as a function of: (a) the waiting time $t_2$ with two different $k_{pt}$ (crosses: 1 ps$^{-1}$ and circles: 0.2 ps$^{-1}$) and pure water (triangles), (b) the PT time scale ($k_{pt}^{-1}$) with two different waiting times $t_2$ (crosses: 1 ps and circles: 5 ps). For comparison, the dashed lines represent the case of pure water.

time to change between the pump and the probe (i.e., during the waiting time), the observed peaks will be extended along the diagonal of the 2DIR spectrum. If the frequency fluctuations are faster than the waiting time, the loss of correlation between the frequency excited at the time of the pump and the frequency detected by the probe, is observed as broadening along the antidiagonal direction, leading to rounder peak shapes. Therefore, if we measure the 2DIR spectra with different waiting times $t_2$, we expect to be able to reveal the value of the PT rate used in the PT model.

The influence of the PT rate on the isotope label 2DIR spectra was investigated further with two different PT rates ($k_{pt} = 1$ and 0.2 ps$^{-1}$) and four different waiting times ($t_2 = 0$, 1, 5, and 10 ps). In Fig. 5, we see that the spectra for both values of $k_{pt}$ are elongated along the diagonal direction for $t_2 = 0$ ps, indicating that little dynamics have taken place. The spectrum with the fast PT ($k_{pt} = 1$ ps$^{-1}$) has a visible increase of the antidiagonal linewidth after $t_2 = 1$ ps, while at $t_2 = 10$ ps all memory is lost. For slow PT ($k_{pt} = 0.2$ ps$^{-1}$) an increased antidiagonal linewidth is seen after $t_2 = 5$ ps, and some memory is still preserved at $t_2 = 10$ ps. This illustrates that, indeed, the behavior of the 2DIR spectrum is sensitive to the PT rate that we set in the model.

We obtained a more quantitative analysis of the 2DIR spectra by calculating the antidiagonal linewidth $\Gamma_{AD}$ as a function of the waiting time $t_2$, as shown in Fig. 6(a). This linewidth is taken as the full width at half maximum (FWHM) of the slice which intersects perpendicularly to the diagonal at the frequency where the linear absorption peak occurs. For $k_{pt} = 1$ ps$^{-1}$, $\Gamma_{AD}$ increases with waiting time $t_2$ from 9.5 cm$^{-1}$ in the beginning and saturates gradually after 5 ps at 14.2 cm$^{-1}$. For $k_{pt} = 0.2$ ps$^{-1}$, $\Gamma_{AD}$ starts at 9 cm$^{-1}$ and still increases after 5 ps where it reaches 12 cm$^{-1}$. Finally, without a proton inside the channel, $\Gamma_{AD}$ becomes saturated already after 2 ps at 11 cm$^{-1}$. These results show that the faster the PT rate is, the faster the anti-diagonal linewidth grows and the quicker it saturates. When there is no proton inside the channel, dynamics is also observed. Then $\Gamma_{AD}$ increases slowly in the beginning, but saturates quickly at a lower value than with a proton in the channel.

To determine how the PT rate changes the time evolution of the 2DIR spectrum in Fig. 5, we plot $\Gamma_{AD}$ as a function of the PT time scale ($k_{pt}{}^{-1}$) at two different waiting times $t_2$ (1 and 5 ps). The pure water (no proton) data are plotted for comparison. The red and blue curves in Fig. 6(b) present exponential fits, given by, respectively:

$$\Gamma_{AD(t_2=1\ ps)} = 11.78\ cm^{-1} - 2.35\ cm^{-1} \times \exp[-0.89\ ps \times k_{pt}], \quad (4)$$

$$\Gamma_{AD(t_2=5\ ps)} = 13.74\ cm^{-1} - 3.43\ cm^{-1} \times \exp[-1.96\ ps \times k_{pt}], \quad (5)$$

where $\Gamma_{AD}$ is measured in $cm^{-1}$. The $\Gamma_{AD}$ of pure water [dashed line in Fig. 6(b)] behave as the asymptotes for the slow PT rates of these two fitting curves. This implies that for the slow PT rates ($k_{pt} \leq 0.1\ ps^{-1}$) the dynamics is essentially identical to that of pure water for these waiting times, and there is no difference observed if the proton is present in the channel or not. The exponential behavior of the antidiagonal width follows from the exponential memory loss seen in the correlation functions, which in turn follows from the fact that we use a kinetic model for the PT. Equations (4) and (5) suggest that measuring the antidiagonal linewidth after a certain waiting time allows the determination of the PT rate.

## IV. DISCUSSION

We have found that the simulated 2DIR spectrum for the kinetic PT model is sensitive to the PT rate that we choose in the model. Our results suggest that in an isotope label 2DIR experiment, the PT rate can be determined by measuring the antidiagonal linewidth of the isotope label peak after a certain waiting time. More specifically, by using Eqs. (4) and (5), a measured value for the antidiagonal linewidth may be translated into an the estimation of the PT rate under confined conditions (inside the channel), showing whether it is faster than the PT rate in bulk water or not. It appears from Fig. 6(a) that the antidiagonal linewidth at low $p$H with proton has a larger value than at neutral $p$H without proton. We cannot directly extract the proton hopping rate by just fitting the $\Gamma_{AD}$ as a function of $t_2$ in Fig. 6(a). The time evolution of the antidiagonal linewidth is entangled with the proton hopping rate and the water diffusion/rotation rates in a complex way. The fast water diffusion (compared to proton hopping) can accelerate the frequency fluctuations, because moving slightly the proton when it is close to the C=O can drastically change the frequency. On the other hand, the water rotation can slow down the frequency fluctuations, because the proton cannot hop unless the neighboring water molecule is in a configuration in which it can accept the proton.

In our PT model, we define a proton entry rate ($k_{pe}$) that is related to the $p$H in the environment and the $pK_a$ of the channel water. We used a uniform PT rate along the channel axis, rather than considering the possibility of position dependent rates. Therefore, the PT rate derived according to our prescription is just the rate of the proton hopping inside the channel near the labeled C=O. In reality the rate found will be the local proton hopping rate or an average value of the position dependent rates in the vicinity of the labeled C=O unit, which depends on the energy surface along channel axis.[24] If the real proton entering process is the rate limiting step for PT ($k_{pe}$ is much smaller than the value used in our model), one may expect that most of the time the dynamics of the system behaves like pure water, because of the very low probability of a proton occurring in the channel, and the 2DIR experiment will only be sensitive at very low $p$H. On the other hand, if the proton exiting or water reorientation processes are the rate limiting steps, the 2DIR experiment can easily be used to determine the average PT rate in the channel, as long as the proton concentration is high enough, and the real PT rate in the channel is in the range between 0.1 $ps^{-1}$ and 2 $ps^{-1}$. If the PT rate is higher than 2 $ps^{-1}$, the system dynamics revealed in the 2DIR spectrum caused by proton hopping will merge with the fast dynamics caused by the protein as seen in Fig. 4(c), and it will be difficult to separate these two processes. If the PT rate is lower than 0.1 $ps^{-1}$, the system dynamics will be difficult to distinguish from the system without protons. Finally, the measurement should be performed at waiting time $t_2$ not much longer than the lifetime of the amide I vibration, because otherwise the 2DIR signal will disappear before the proton can move.

It is important to address the question whether or not the effects predicted with our PT model can be resolved in experimental 2DIR spectra. We expect that the real PT rate in the channel is comparable to that found in liquid water (from 0.67 $ps^{-1}$ to 1.2 $ps^{-1}$).[54,55] These PT rates are within the limits of our model and the PT time scale is not too long compared with the amide I vibrational lifetime. In typical 2DIR experiments the linewidth resolution is 0.5 $cm^{-1}$,[28,56] and the time dependent change found in our model should be easily observed. Therefore, it is realistic that one can obtain the PT rate from 2DIR experiments even the estimated PT rate will of course be subject to an error bar that can be reduced by improving the resolution of the experiment and by improving the models used for simulating the spectra.

In our model we do not account for the fact that the protein structure might be affected by the presence of the proton. Previous simulation studies have shown that such effect is indeed small.[57] However, it can not be completely excluded that there will be some effect of protein reorganization on the spectra. Future studies explicitly including the proton will be able to elucidate this issue.

## V. CONCLUSIONS

In this paper, we constructed a kinetic PT model, parametrized from all-atom MD simulations, that describes the proton transport process in the gA channel. This model allowed us to simulate 2DIR spectra of isotope labeled C=O stretch vibrations in the peptide and analyze the effect of PT on the spectra. By varying the intermolecular PT rate in the model we observed that the antidiagonal linewidth of the 2DIR spectrum is sensitive to this rate. We therefore propose that measuring this linewidth as a function of waiting time can be used as an experimental tool to determine the intermolecular PT rate in biological channels.

We found that the rate of the time evolution of the antidiagonal linewidth is *not* equal to the proton hopping rate, but is determined by a complex interplay between this quantity, the water reorientation rate, and the water diffusion constant. To extract the local proton hopping rate, it is therefore necessary to compare with theory. From our model we found a relation between the spectral behavior and the actual PT rate. In the future more advanced models based on PT methods such as Q-HOP[58] or MS-EVB,[59] should enable one to verify or possibly improve this relationship.

Our method strictly speaking only applies to residue four of gA, for which it was parameterized. However, one can expect that the most important contributions to the frequency fluctuations that arise from the electric fields generated by the proton and the water are only weakly depending on the site. This again should be addressed in future studies explicitly including a proton and looking at the effect at different sites. The method should be applicable to other proteins involved in PT as well, but numerical simulations will be needed to interpret the spectra.

With existing experimental methods only the overall proton conductance in a channel can be measured. With our proposal it should be possible to measure the proton hopping rate between two water molecules. By isotope labeling different sites it should be possible to determine the hopping rate at different positions. In this way one will be able to find possible bottlenecks within a channel, which is impossible with the existing single channel conductance experiments. This will be a crucial step in determining the relative importance of different processes in the proton conduction through channel proteins, which is impossible when only the overall proton conductance is measured. In combination with protein mutation, lipid length/bilayer thickness, or other alterations, our method may also elucidate which role these parts of the environment play in the overall process. Such measurements should be supported by detailed numerical simulations.

## ACKNOWLEDGMENTS

TLCJ acknowledges the Netherlands Organization for Scientific Research (NWO) for support through a VIDI grant. The authors thank Dr. G. Portella for helping with the Gramicidin A topology file for GROMACS.

[1] C. J. T. de Grotthuss, Ann. Chim. **58**, 54ð73 (1806).
[2] N. Agmon, Chem. Phys. Lett. **224**, 456 (1995).
[3] J. D. Bernal and R. H. Fowler, J. Chem. Phys. **1**, 515 (1933).
[4] K. J. Tielrooij, R. L. A. Timmer, H. J. Bakker, and M. Bonn, Phys. Rev. Lett. **102**, 198303 (2009).
[5] O. S. Andersen, Annu. Rev. Physiol. **46**, 531 (1984).
[6] B. A. Wallace, Annu. Rev. Biophys. Chem. **19**, 127 (1990).
[7] R. E. Koeppe and O. S. Andersen, Annu. Rev. Biophys. Biomech. **25**, 231 (1996).
[8] A. Chernyshev and S. Cukierman, Biophys. J. **82**, 182 (2002).
[9] B. Roux and M. Karplus, Annu. Rev. Biophys. Biomol. Struct. **23**, 731 (1994).
[10] T. B. Woolf and B. Roux, Proteins Struct. Funct. Genet. **24**, 92 (1996).
[11] R. Pome and B. Roux, Biophys. J. **82**, 2304 (2002).
[12] B. L. de Groot, D. P. Tieleman, P. Pohl, and H. Grubmuller, Biophys. J. **82**, 2934 (2002).
[13] T. Bastug, A. Gray-Weale, S. M. Patra, and S. Kuyucak, Biophys. J. **90**, 2285 (2006).
[14] A. S. Bourinbaiar and C. F. Coleman, Archives of Virology **142**, 2225 (1997).
[15] C. Dellago, M. M. Naor, and G. Hummer, Phys. Rev. Lett. **90**, 105902 (2003).
[16] D. J. Mann and M. D. Halls, Phys. Rev. Lett. **90**, 195503 (2003).
[17] M. S. Till, T. Essigke, T. Becker, and G. M. Ullmann, J. Phys. Chem. B **112**, 13401 (2008).
[18] N. Agmon, J. Chem. Phys. **93**, 1714 (1996).
[19] S. Braun-Sand, A. Burykin, Z. T. Chu, and A. Warshel, J. Phys. Chem. B **109**, 583 (2005).
[20] S. W. Chiu, S. Subramaniam, and E. Jakobsson, Biophys. J. **76**, 1939 (1999).
[21] M. Schumaker, Front. Biosci. **8**, s982 (2003).
[22] D. L. Wyatt, C. M. de Godoy, and S. Cukierman, J. Phys. Chem. B **113**, 6725 (2009).
[23] M. Akeson and D. W. Deamer, Biophys. J. **60**, 101 (1991).
[24] G. Portella, P. Pohl, and B. L. de Groot, Biophys. J. **92**, 3930 (2007).
[25] G. Portella and B. L. de Groot, Biophys. J. **96**, 925 (2009).
[26] G. A. Voth, Acc. Chem. Res. **39**, 143 (2006).
[27] C. A. Wraight, Biochim. Biophys. Acta **1757**, 886 (2006).
[28] J. B. Asbury, T. Steinel, K. Kwak, S. A. Corcelli, C. P. Lawrence, J. L. Skinner, and M. D. Fayer, J. Chem. Phys. **121**, 12431 (2004).
[29] T. L. C. Jansen and J. Knoester, Acc. Chem. Res. **42**, 1405 (2009).
[30] Y. S. Lin, J. M. Shorb, P. Mukherjee, M. T. Zanni, and J. L. Skinner, J. Phys. Chem. B **113**, 592 (2009).
[31] M. Cho, Chem. Rev. **108**, 1331 (2008).
[32] W. Zhuang, T. Hayashi, and S. Mukamel, Angew. Chem. Int. Ed. **48**, 3750 (2009).
[33] S. Park, M. Odelius, and K. J. Gaffney, J. Phys. Chem. B **113**, 7825 (2009).
[34] S. Bagchi, A. K. Charnley, A. B. Smith, and R. M. Hochstrasser, J. Phys. Chem. B **113**, 8412 (2009).
[35] S. Woutersen and P. Hamm, J. Chem. Phys. **115**, 7737 (2001).
[36] N. Demirdöven, C. M. Cheatum, H. S. Chung, M. Khalil, J. Knoester, and A. Tokmakoff, J. Am. Chem. Soc. **126**, 7981 (2004).
[37] A. W. Smith, H. S. Chung, Z. Ganim, and A. Tokmakoff, J. Phys. Chem. B **109**, 17025 (2005).
[38] P. Hamm, M. H. Lim, and R. M. Hochstrasser, J. Phys. Chem. B **102**, 6123 (1998).
[39] P. Mukherjee, A. T. Krummel, E. C. Fulmer, I. Kass, I. T. Arkin, and M. T. Zanni, J. Chem. Phys. **120**, 10215 (2004).
[40] T. L. C. Jansen and J. Knoester, J. Chem. Phys. **124**, 044502 (2006).
[41] T. L. C. Jansen and J. Knoester, J. Phys. Chem. B **110**, 22910 (2006).
[42] E. Lindahl, B. Hess, and D. van der Spoel, J. Mol. Mod. **7**, 306 (2001).
[43] W. L. Jorgensen and J. Tirado-Rives, J. Am. Chem. Soc. **110**, 1657 (1988).
[44] D. P. Tieleman, J. L. MacCallum, W. L. Ash, C. Kandt, Z. Xu, and L. Monticelli, J. Phys. Cond. Matt. **18**, S1221 (2006).
[45] W. L. Jorgensen, J. Chandrasekhar, J. D. Madura, R. W. Impey, and M. L. Klein, J. Chem. Phys. **79**, 926 (1983).
[46] L. E. Townsley, W. A. Tucker, S. Sham, and J. F. Hinton, Biochemistry **40**, 11676 (2001).
[47] C. Kandt, W. L. Ash, and D. P. Tieleman, Methods **41**, 475 (2007).
[48] See supplementary material at http://dx.doi.org/10.1063/1.3522770 for details on the all-atom simulations and the parameterization of the kinetic model.
[49] T. L. C. Jansen, A. G. Dijkstra, T. M. Watson, J. D. Hirst, and J. Knoester, J. Chem. Phys. **125**, 44312 (2006).
[50] D. E. Sagnella, K. Laasonen, and M. L. Klein, Biophys. J. **71**, 1172 (1996).
[51] J. D. Hybl, Y. Christophe, and D. M. Jonas, Chem. Phys. **266**, 295 (2001).
[52] S. T. Roberts, J. J. Loparo, and A. Tokmakoff, J. Chem. Phys. **125**, 084502 (2006).
[53] K. Kwak, D. E. Rosenfeld, and M. D. Fayer, J. Chem. Phys. **128**, 204505 (2008).
[54] Z. Luz. and S. Meiboom, J. Am. Chem. Soc. **86**, 4768 (1964).
[55] B. J. Siwick, M. J. Cox, and H. J. Bakker, J. Phys. Chem. B **112**, 378 (2008).
[56] P. Mukherjee, I. Kass, I. T. Arkin, and M. T. Zanni, Proc. Natl. Acad. Sci. USA **103**, 3528 (2006).
[57] R. Pomés and B. Roux, Biophys. J. **71**, 19 (1996).
[58] M. A. Lill and V. Helms, J. Chem. Phys. **115**, 7993 (2001).
[59] U. W. Schmitt and G. A. Voth, Chem. Phys. Lett. **329**, 36 (2000).